RSC Advances

PAPER

View Article Online
View Journal | View Issue

Cite this: *RSC Adv.*, 2022, **12**, 11906

Metal chloride anion based ionic liquids: synthesis, characterization and evaluation of performance in hydrogen sulfide oxidative absorption†

Muhammad Syahir Aminuddin, [a] Mohamad Azmi Bustam Khalil[b] and Bawadi Abdullah *[c]

Received 7th March 2022
Accepted 1st April 2022

DOI: 10.1039/d2ra01494g

rsc.li/rsc-advances

Three metal chloride anion based ionic liquids (MCABILs) were synthesized and characterized for high conversion of hydrogen sulfide (H_2S). The MCABILs were synthesized *via* metathesis reaction and characterized by chemical spectroscopy such as FTIR, UV-Vis and CHNS elemental analysis. Then, the performance of those ionic liquids in H_2S conversion was evaluated at various temperatures and atmospheric pressure. The results indicated remarkable efficiency of metal chloride anion based ionic liquids in H_2S conversion. MCABILs managed to reach over 90% conversion efficiency at temperature as low as 50 °C, despite operating at atmospheric pressure. This occurs due to their high oxidation capability. The regeneration experiment indicated that all MCABILs can be recycled easily. Taken together, the research findings highlight the synthesis, characterization and high efficiency of MCABILs in promoting faster H_2S conversion as a catalyst.

1. Introduction

H_2S is a colorless gas that exists naturally,[1] and is very toxic[2] and highly flammable. Its harmful effects towards living organisms are visible at 10 ppm (ref. 3) and become fatal after exceeding 500 ppm.[4] H_2S is also highly corrosive to carbon steel.[5] Thus, H_2S removal is very crucial for economic and safety reasons. Absorption, adsorption and conversion are common desulphurization technologies. LO-CAT and Claus process are most outstanding as they are capable of converting H_2S into sulfur with excellent efficiency.[6] However, they consume a lot of energy and face catalyst deactivation. Consequently, sulfur production output is lowered and cost increased.[7] Ionic liquids (ILs) are salts with melting point lower than the water boiling point and have emerged as promising green solvents for desulphurization.[8] ILs are designer solvents because their physicochemical properties are tunable by changing the cation and anion.[9] Hence, they can be designed specifically for desulphurization. Recently, many studies were targeting H_2S conversion into sulfur using ILs.[10–14] Since there are unlimited possible combinations, evaluation for most efficient ILs would be very tedious and costly if carried out experimentally.[15,16] The chances to discover and select new ILs would be complicated. Thus, every potential IL must undergo a thorough and systematic screening.

This work is a continuation study of screening potential ILs for direct conversion of H_2S by Conductor-like Screening Model for Real Solvents (COSMO-RS).[17] COSMO-RS screening was conducted to predict the thermodynamic properties of ILs for H_2S conversion without requiring any prior experimental data. Based on COSMO-RS prediction, economical and safety reasons, three MCABILs were selected for synthesis from 300 screened.[17] Various studies have discovered potential Room-Temperature Ionic Liquids (RTILs) application for H_2S conversion,[18,19] nonetheless, it is discovered that their capacity and solubility for H_2S are still poor at low pressure.[20–23] Thus, this study was performed using Task Specific Ionic Liquids (TSILs) which is MCABILs that were improved[24,25] and capable of promoting faster H_2S conversion to sulfur.[11,26] Three selected ILs were; trihexyl(tetradecyl)phosphonium tetrachlorogallate, $[P_{66614}][GaCl_4]$, trihexyl(tetradecyl)phosphonium tetrachloroferrate, $[P_{66614}][FeCl_4]$ and trihexyl(tetradecyl)phosphonium trichlorostannate, $[P_{66614}][SnCl_3]$.

2. Materials and methods

2.1. Materials

Trihexyl(tetradecyl)phosphonium chloride, $[P_{66614}][Cl]$ of 95% purity was purchased from Sigma-Aldrich. The metal chlorides used for this work were gallium(III) chloride, iron(III) chloride and tin(II) chloride. Gallium(III) chloride, $GaCl_3$ of 99.999%

[a]Department of Chemical Engineering, Universiti Teknologi PETRONAS, 32610 Bandar Seri Iskandar, Perak, Malaysia

[b]Centre of Research in Ionic Liquids (CORIL), Universiti Teknologi PETRONAS, 32610 Bandar Seri Iskandar, Perak, Malaysia

[c]Centre of Contamination Control and Utilization (CenCoU), Universiti Teknologi PETRONAS, 32610 Bandar Seri Iskandar, Perak, Malaysia. E-mail: bawadi_abdullah@utp.edu.my; bawadi73@gmail.com

† Electronic supplementary information (ESI) available. See https://doi.org/10.1039/d2ra01494g

purity, anhydrous iron(III) chloride, $FeCl_3$ of 97% purity and tin(II) chloride, $SnCl_2$ of 98% purity were also purchased from Sigma-Aldrich. All chemicals used are analytical grade and require no purification.

2.2. Synthesis of MCABILs

Three MCABILS were synthesized by metathesis reaction of $[P_{66614}][Cl]$ with $GaCl_3$, $FeCl_3$ an $SnCl_2$ to produce trihexyltetradecylphosphonium tetrachlorogallate, $[P_{66614}][GaCl_4]$, trihexyltetradecylphosphonium tetrachloroferrate, $[P_{66614}][FeCl_4]$ and trihexyltetradecylphosphonium trichlorostannate, $[P_{66614}][SnCl_3]$. $[P_{66614}][GaCl_4]$ was synthesized by metathesis reaction according to Fig. 1.

$P_{66614}Cl$ and $GaCl_3$ were reacted in round bottom flask with stirrer to ensure uniform heating and perfect mixing at 25 °C for 24 h. The product was filtered and washed with deionized water to remove unwanted salt and impurities. To minimise water content and volatiles to lowest possible values, the synthesized MCABILs underwent rotary evaporation at 70 °C in vacuum condition for several days. The procedure were repeated with $[P_{66614}][FeCl_4]$ and $[P_{66614}][SnCl_3]$.

$[P_{66614}][GaCl_4]$ formed was a dark red liquid. The yield obtained was 99.0% and the water content was measured at 11 ppm. CHNS analysis calculated (found); C: 55.27 (55.24), H: 9.86 (9.89), N: 0 (0), S: 0 (0).

$[P_{66614}][FeCl_4]$ was formed was a dark black liquid. The yield for $[P_{66614}][FeCl_4]$ was 96.7% and the water content was obtained at 17 ppm. CHNS analysis calculated (found); C: 56.40 (56.38), H: 10.06 (10.09), N: 0 (0), S: 0 (0).

$[P_{66614}][SnCl_3]$ was obtained as a golden yellow colour liquid. The product yield was 90.3% and the water content was found to be at 25 ppm. CHNS analysis calculated (found); C: 54.22 (54.19), H: 9.67 (9.71), N: 0 (0), S: 0 (0).

2.3. Characterization instruments

CHNS elemental analysis was performed using Leco-CHNS-932 Analyzer. FT-IR spectra of the samples were collected by Fourier transfrom infrared Thermo Nicolet is5 spectrometer. TGA curve was obtained by PerkinElmer thermogravimetric analyzer, Pyris V-3.81. DSC curve was collected by DSC Q2000 V24.11 Build 124 (Universal V4.5A TA Instruments). Density was determined by density meter DA-645 (Kyoto Electronics Manufacturing). Viscosity was obtained by AMVn Anton Paar micro viscometer. The water content analyses were conducted by V30 Mettler Toledo coulometric Karl Fischer titrator.

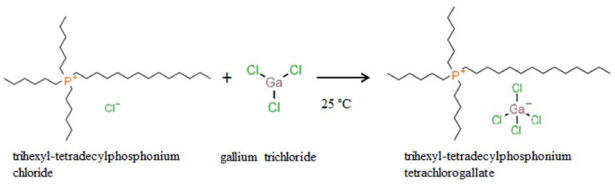

Fig. 1 Reaction mechanism for synthesis of trihexyl(tetradecyl)phosphonium tetrachlorogallate, $[P_{66614}][GaCl_4]$.

2.4. H_2S absorption measurement

H_2S absorption measurement was conducted at atmospheric pressure and various temperatures at 25 °C, 50 °C, 75 °C and 100 °C as depicted in Fig. 2. Raw materials inlet into the system consists of three gas path way and the gas flow rate was controlled by the flow meter and mass flow controller. A gas mixture of oxygen and 100 ppm concentration of H_2S was passed through the 25 mL stainless steel reactor in which the MCABILs were loaded. N_2 gas was used as the carrier gas and purging gas to ensure all the system is free of H_2S before and after the reaction happened. The reaction temperature was between room temperature until 100 °C and regulated by the heating mantel around the reactor. The concentration of H_2S at both inlet and outlet gas was detected by H_2S gas analyzers. The residual H_2S gas was absorbed by the concentrated NaOH solution in the scrubber tanks. In this test, a maximum 10 ppm of the initial concentration of H_2S was defined as the breakthrough concentration.

3. Results and discussion

3.1. FT-IR spectra of MCABILs

The infrared spectra of $[P_{66614}][GaCl_4]$, $[P_{66614}][FeCl_4]$ and $[P_{66614}][SnCl_3]$ display several peaks at 1465 cm^{-1}, 1410 cm^{-1}, 1110 cm^{-1} and 720 cm^{-1} associated with P–C stretching vibration as depicted in Fig. 3. The broad peak that exists in region between 2960 cm^{-1} to 2850 cm^{-1} are assigned to aliphatic moieties of C–H stretching vibration. The bands located at 985 cm^{-1} and 810 cm^{-1} are attributed to CH=CH bending vibrations. A single peak at 1375 cm^{-1} is associated with CH_2–CH_3 stretching vibration, while the peak at 1210 cm^{-1} is corresponded to C–H bending vibration. Based on spectra analysis, there is no presence of alkyl halides, C–Cl bond. Hence, this confirms the structure of MCABILs as shown in Fig. S1–S3.†

3.2. Density and viscosity of MCABILs

Fig. 4(a) and (b) show the density and viscosity of MCABILs, respectively. The densities varied from 0.98139 to 1.05059 g cm^{-3} and in reported range of 0.9 to 1.7 g cm^{-3}.[27] No significant decrease in viscosity was observed after the temperature reached 60 °C.[28] The viscosity and density of

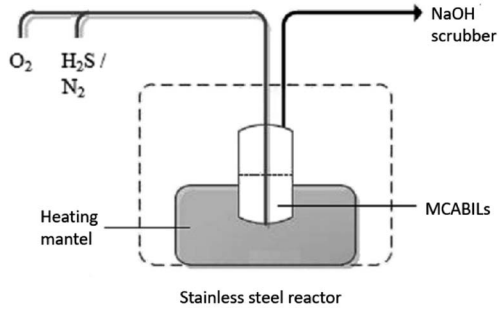

Fig. 2 Schematic diagram for H_2S oxidative absorption experimental set up.

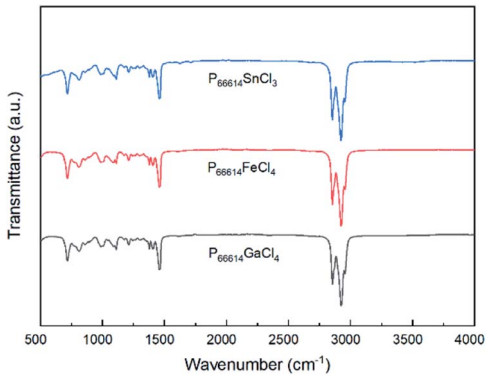

Fig. 3 FTIR spectra of MCABILs: $[P_{66614}][GaCl_4]$, $[P_{66614}][FeCl_4]$ and $[P_{66614}][SnCl_3]$.

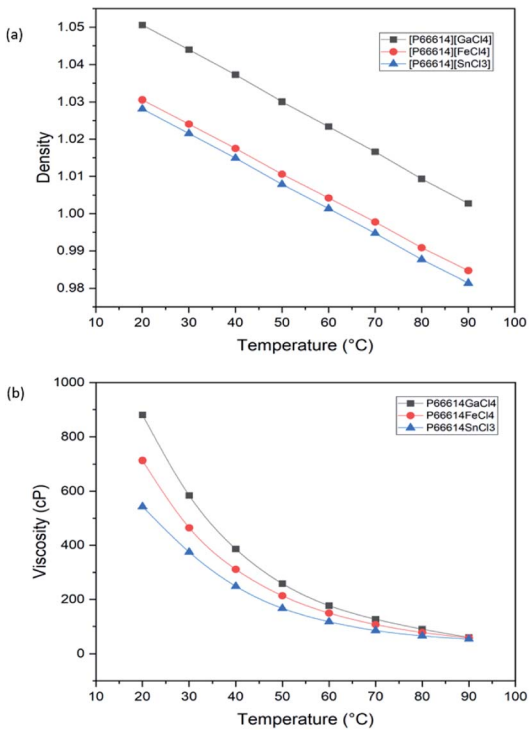

Fig. 4 The relationship between (a) density and (b) viscosity *versus* temperature for all MCABILs.

MCABILs decrease as the temperature increases. At 20 °C, MCABILs exhibited viscosity between 543.11 to 880.42 cP and density between 0.98139 and 1.00274 g cm^{-3} as shown in Tables S1 and S2.† Since MCABILs possess lower viscosity and density at higher temperature, they can be excellent catalysts for direct H_2S conversion.

3.3. TGA and DSC analysis of MCABILs

Fig. 5(a) and (b) represent the TGA and DSC curves of MCABILs, respectively. Thermal stability for each ILs was reported as thermal onset and decomposition temperatures in Table S3.† The decomposition temperature has appeared at 480.34 °C, 478.57 °C and 468.77 °C for $[P_{66614}][GaCl_4]$, $[P_{66614}][FeCl_4]$ and $[P_{66614}][SnCl_3]$, respectively. These ILs display high thermal stability and $[P_{66614}][GaCl_4]$ being the most stable. They were fully decomposed at a high temperature of 500 °C because phosphonium based ILs are very stable thermally.[29] Since each MCABILs possesses T_{onset} higher than 400 °C, it is concluded that each of them is very stable ILs thermally.[30] The melting point for each MCABILs are shown in Table S4.† The melting points of MCABILs increases as the molecular weight (MW) of the anions increases. An increase in MW of the anions side chains resulted in stronger intermolecular reaction which contributes to the rise in melting points. Since they share similar cation, the melting points only vary slightly.

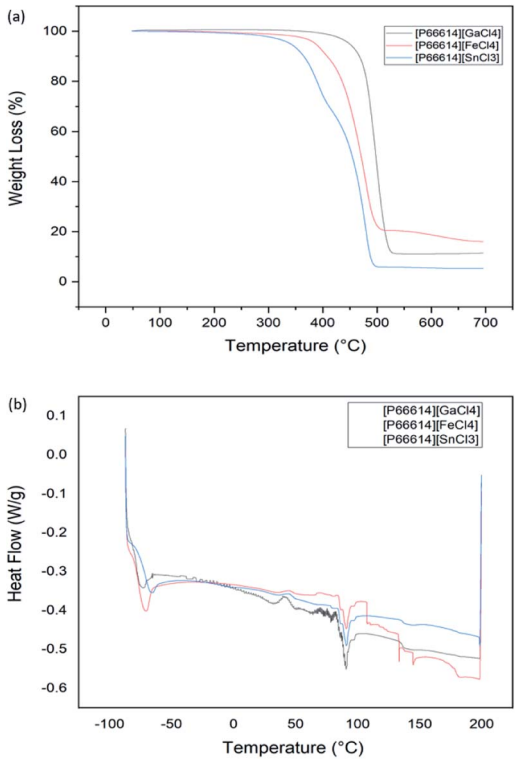

Fig. 5 (a) TGA and (b) DSC profiles of MCABILs.

3.4. H_2S removal performance of MCABILs

As depicted in Table 1, the efficiencies of H_2S removal for all three MCABILs increased to over 90% within 360 min (6 h) at 100 °C. This indicates high performance and H_2S conversion capabilities in those ILs. Among all three MCABILs, $P_{66614}GaCl_4$ demonstrated a lower H_2S absorption capability compared to

Table 1 Desulfurization performance of MCABILs after 6 h

Ionic liquids	Percentage of H_2S removal after 6 h at 100 °C (%)
$P_{66614}GaCl_4$	92.23
$P_{66614}FeCl_4$	93.51
$P_{66614}SnCl_3$	97.54

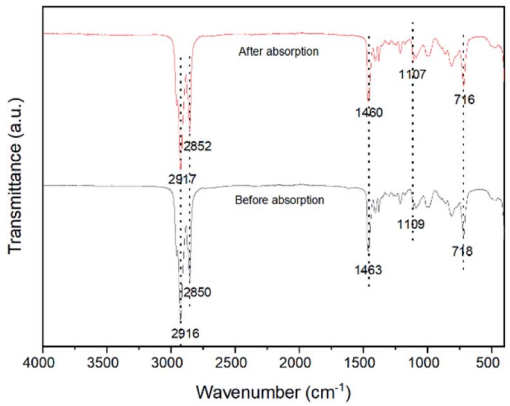

Fig. 6 FT-IR spectra of MCABILs before and after H_2S absorption

the other two MCABILs. Ding *et al.*[26] designed a series of TSILs containing metal chelate cations for SO_2 capture. The results indicated that SO_2 solubility increases with the increase of metal ion radius and decreasing acidity due to alkali metal ion. According to Wang & Zhang,[31] metal containing ILs are capable of absorbing H_2S efficiently under certain pressure. They also stated that the metal anions acidity plays an important factor for H_2S absorption.

In this work, H_2S absorption was performed in dynamic conditions and the partial pressure was also relatively low. However, the MCABILs were still able to perform well while maintaining high efficiency of H_2S removal at relatively low pressure. The H_2S conversion percentages were calculated using eqn (1):

$$H_2S\ \text{conversion}\ (\%) = \frac{x_{H_2S,in} - x_{H_2S,out}}{x_{H_2S,in}} \times 100 \quad (1)$$

where, $x_{H_2S,in}$ and $x_{H_2S,out}$ are the concentration of H_2S at the inlet and outlet, respectively.

Fig. 6 depicted the FT-IR spectra of MCABILs before and after H_2S conversion. Since it does not show any significant difference, that means no chemical reaction between H_2S and ILs molecules have occurred. The presence of metal chlorides in the ILs matrix enhance the desulfurization abilities of pure ILs which have low physical and chemical solubility of H_2S.

3.5. Mechanism of absorption

The reaction mechanism of H_2S oxidative absorption in this research involves redox reaction between MCABILs and H_2S. A study conducted by DeBerry *et al.*[32] revealed that $Fe(III)Cl_4^-$ was reduced to $Fe(III)Cl_4^-$ during H_2S oxidation in DMSO. In this work, the metal chloride anions in the ILs was reduced while H_2S is being oxidized simultaneously. By combining the present work with research conducted by Nguyen *et al.*,[33] the complete reaction mechanism for absorptive oxidation by one of the MCABILs is depicted as eqn (2) and (3).

$$[P_{66614}]GaCl_4 + H_2S \rightarrow ([P_{66614}]GaCl_3)^* + S_8 + HCl \quad (2)$$

$$([P_{66614}]GaCl_3)^* + HCl \rightarrow [P_{66614}]GaCl_4H \quad (3)$$

The reaction began with the reduction of $\{P_{66614}]GaCl_4$ into $([P_{66614}]GaCl_3)^*$ by H_2S. $([P_{66614}]GaCl_3)^*$ was an intermediate species that reacted with HCl instantaneously to form $[P_{66614}]GaCl_4H$. The hydrogen ion in $[P_{66614}]GaCl_4H$ is most likely to react with Cl^- in MCABILs to form HCl, resulting in a strong acidic environment. The regeneration of MCABILs was performed by bubbling N_2 gas through the catalyst for approximately 3 h.

3.6. Factors affecting H_2S removal performance of the MCABILs

3.6.1. Effects of absorption temperature. The H_2S conversion performance for one of MCABILs, $P_{66614}FeCl_4$ at different temperatures is shown in Fig. 7. The result reported a higher conversion at higher temperature. This demonstrates that the conversion of H_2S is an endothermic reaction, which is supported by literature.[34] Since it is an endothermic process, it limits the thermodynamic conversion at lower temperature.

However, since MCABILs were designed specifically to perform excellently at low temperature and pressure, MCABILs still can achieve high conversion as high as 90% at 50 °C and 1 atm. At higher temperature, the conversion of H_2S in MCABILs is much higher. It can be concluded that the performance of MCABILs is optimum at higher temperature.

3.6.2. Effects of viscosity of MCABILs. Tables 2 and 3 shows the desulfurization performance of MCABILs with respect to their viscosity at 50 °C and 100 °C, respectively. Among all three MCABILs, $P_{66614}GaCl_4$ demonstrated a lower H_2S conversion at lower temperature. This is because $P_{66614}GaCl_4$ has the highest viscosity followed by $P_{66614}FeCl_4$ and $P_{66614}SnCl_3$. It is very viscous at lower temperature and unable to perform the conversion efficiently. Meanwhile, $P_{66614}SnCl_3$ which possess a low viscosity at lower temperature showed a remarkable performance in H_2S conversion. Hence, lower viscosity ILs are the best choice for H_2S conversion.

3.6.3. Effects of reaction with time. Fig. 8 shows the percentage of H_2S conversion into elemental sulfur with respect to reaction time, using $P_{66614}FeCl_4$. At the beginning, the reaction was rather slow because of mixing and dispersion of H_2S,

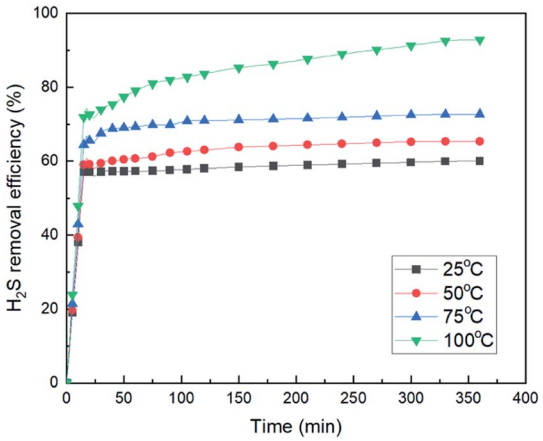

Fig. 7 Desulfurization performance of MCABILs, $P_{66614}FeCl_4$ at different temperature.

Table 2 Desulfurization performance and viscosity of MCABILs at 50 °C after 6 h

Ionic liquids	Viscosity (cp)	Conversion (%)
$[P_{66614}][GaCl_4]$	258.37	65.35
$[P_{66614}][FeCl_4]$	213.41	69.03
$[P_{66614}][SnCl_3]$	167.17	91.75

Table 3 Desulfurization performance and viscosity of MCABILs at 100 °C after 6 h

Ionic liquids	Viscosity (cp)	Conversion (%)
$[P_{66614}][GaCl_4]$	59.43	92.23
$[P_{66614}][FeCl_4]$	57.96	93.51
$[P_{66614}][SnCl_3]$	53.42	97.54

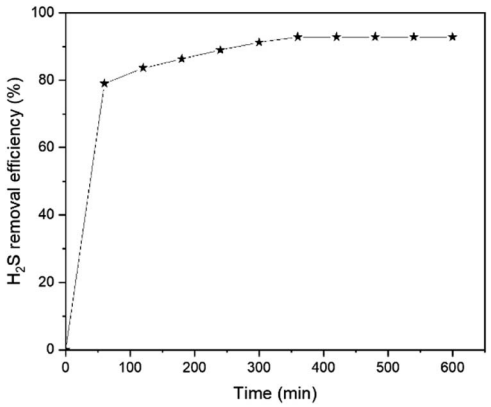

Fig. 8 The effect of reaction time on H_2S conversion using MCABILs, $P_{66614}FeCl_4$ at 100 °C.

O_2 and ILs phases. For example, conversion of H_2S into elemental sulfur by $P_{66614}FeCl$ at 100 °C and 1 bar. The obtained results were 79.07%, 83.69%, 86.4%, 88.94%, 91.25% and 92.83% at 60, 120, 180, 240, 300 and 360 min respectively. The conversion rate increases with time because of the increase in mass transfer between the mixture gases of H_2S and O_2 and the catalyst, metal chloride anion based ILs and completed after a certain period of time.

Liu and Wang[35] reported that as the reaction was prolonged until 10 h, the percentage of H_2S conversion in $PMo_{10}V_2$/BmimCl decreases to below 75% which demonstrated that $PMo_{10}V_2$/BmimCl is only acting as solvent. Meanwhile, MCABILs maintains a high conversion percentage above 90% until 600 min without any performance drop and signifies its role as a catalyst for desulfurization reaction.

The experimental results indicated that the percentage of conversion (%) increases with increasing reaction time. As the reaction reaches 360 min, the conversion percentage of H_2S has reached its peak at 93.51% and remain stagnant afterwards until reaches 600 min. Hence, 360 min can be deduced as the optimum reaction time for conversion of H_2S into elemental sulfur.

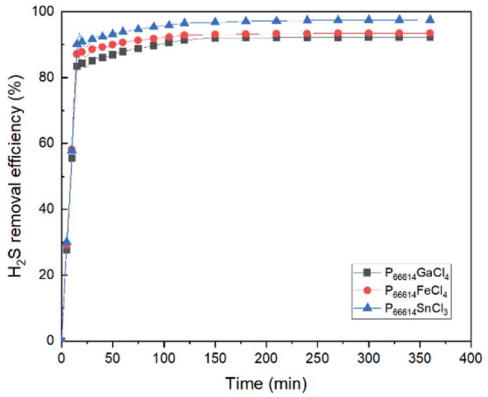

Fig. 9 Comparison of desulfurization performance of MCABILs at 100 °C for 6 h.

3.7. Comparison of desulfurization performance for MCABILs

As shown in Fig. 9, all MCABILs with phosphonium cations demonstrated a high rate of desulfurization, reaching above 90% during 6 h of reaction at 100 °C. The performance of all MCABILs at 50 °C were also depicted in Fig. 10. Comparatively, the performance of MCABILs at lower temperature were a bit lower compared to their performance at 100 °C. This is probably due to higher viscosity of MCABILs at lower temperature.

Since MCABILs consist of similar cation, it is concluded that the metal chloride anions and their oxidation number play a significant role in affecting the desulfurization performance. MCABILs were playing role as catalysts for the removal of H_2S through absorptive oxidation. Comparatively, they are more stable and efficient compared to the conventional ILs reported[36,37] under similar operating conditions.

Among three MCABILs, $P_{66614}SnCl_3$ is the best catalyst for H_2S absorptive oxidation with removal rate of 97.54%. The sequence of H_2S removal efficiencies of MCABILs are in the following order of $[P_{66614}][SnCl_3]$ > $[P_{66614}][FeCl_4]$ > $[P_{66614}][GaCl_4]$. The efficiencies of MCABILs for H_2S removal increased

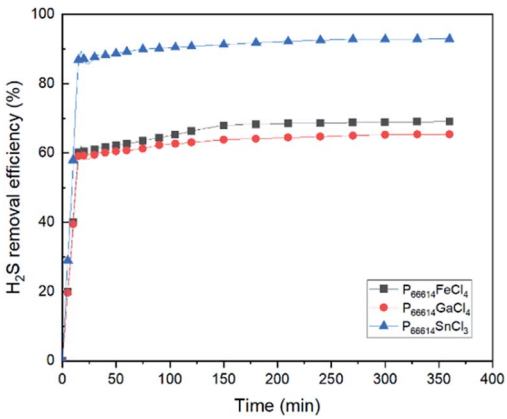

Fig. 10 Comparison of desulfurization performance of MCABILs at 50 °C for 6 h.

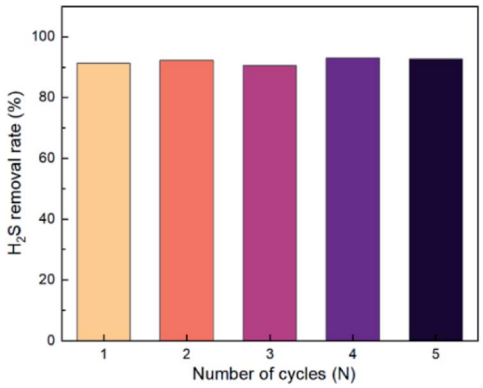

Fig. 11 Regeneration performance of MCABILs, $P_{66614}FeCl_4$.

as the viscosity of MCABILs decreased. As a result, $P_{66614}SnCl_3$ demonstrated the best desulfurization performance.

3.8. Regeneration performance of MCABILs

MCABILs can be regenerated by flowing N_2 at 200 mL min^{-1} for 30 min at 50 °C. The MCABILs used to study regeneration process was $[P_{66614}][FeCl_4]$. The regeneration performance of MCABILs was depicted in Fig. 11. The efficiency of H_2S removal was observed after the absorption took place for 3 h. The rates of H_2S removal for the studied MCABILs were found to be higher than 90% within 5 cycles thus, signifying an outstanding regeneration performance of MCABILs for H_2S removal.

4. Conclusions

The contribution of this paper is twofold; to report the synthesis and characterization of three new MCABILs *via* combination of trihexyl(tetradecyl)phosphonium cation with metal chloride-anions and to evaluate their performance in H_2S conversion. The yields for all ionic liquids were obtained in range of 90% to 99%. The synthesized ILs exist as liquid at room temperature and very stable thermally, possessing high decomposition temperatures ranging between 468.77 °C and 480.34 °C. Overall, MCABILs show desirable physical properties which make them excellent catalysts for absorptive oxidation of H_2S. Those MCABILs also shown a remarkable desulfurization performance with over 90% efficiency at atmospheric pressure and can be regenerated for multiple usage.

Abbreviations

CHNS	Carbon, hydrogen, nitrogen, sulphur
DSC	Differential scanning calorimetry
FT-IR	Fourier transformed infrared
H_2S	Hydrogen sulfide
ILs	Ionic liquids
MCABILs	Metal chloride anion based ionic liquids
RTILs	Room temperature ionic liquids
TGA	Thermogravimetric analysis
TSILs	Task specific ionic liquids

Author contributions

Muhammad Syahir Aminuddin: conceptualization, methodology, investigation, writing – original draft. Mohamad Azmi Bustam: supervision, validation. Bawadi Abdullah: supervision, funding acquisition, validation, writing – review & editing.

Conflicts of interest

There are no conflicts to declare.

Acknowledgements

The authors acknowledge the funding for research work from Yayasan Universiti Teknologi PETRONAS (YUTP) under the YUTP-FRG Scheme (015LC0-263), Universiti Teknologi PETRONAS (UTP).

Notes and references

1 E. Total, *Sour Gas, A History of Expertise, Group*, 2007, vol. 24.
2 A. J. Kidnay, W. R. Parrish and D. G. McCartney, *Fundamentals of natural gas processing*, CRC Press, 2019.
3 P. C. Database, *Hydrogen sulfide*, **https://pubchem.ncbi.nlm.nih.gov/compound/Hydrogen-sulfide**, accessed September 4, 2020.
4 O. S. a. H. Administration, *Safety and Health Topics/Hydrogen Sulfide*, **https://www.osha.gov/SLTC/hydrogensulfide/hazards.html**, accessed September 4, 2020.
5 M. Shahid and M. Faisal, *Arabian J. Sci. Eng., Sect. A*, 2009, **34**, 179.
6 M. J. Goodwin, O. M. Musa and J. W. Steed, *Energy Fuels*, 2015, **29**, 4667–4682.
7 M. Abdul Aziz and A. Mithani, *Holistic Approach in Managing Challenges of Mature Offshore Carbonate Gas Fields with High CO_2 and H_2S Content in Sarawak Gas Operations*, Society of Petroleum Engineers, Malaysia, 2017.
8 K. Huang, X. Feng, X.-M. Zhang, Y.-T. Wu and X.-B. Hu, *Green Chem.*, 2016, **18**, 1859–1863.
9 X. Wang, S. Zeng, J. Wang, D. Shang, X. Zhang, J. Liu and Y. Zhang, *Ind. Eng. Chem. Res.*, 2018, **57**, 1284–1293.
10 D. Shang, X. Liu, L. Bai, S. Zeng, Q. Xu, H. Gao and X. Zhang, *Curr. Opin. Green Sustainable Chem.*, 2017, **5**, 74–81.
11 B. Guo, E. Duan, Y. Zhong, L. Gao, X. Zhang and D. Zhao, *Energy Fuels*, 2011, **25**, 159–161.
12 Y. Ma, X. Liu and R. Wang, *J. Hazard. Mater.*, 2017, **331**, 109–116.
13 M. Li, J. Guan, J. Han, W. Liang, K. Wang, E. Duan and B. Guo, *J. Mol. Liq.*, 2015, **209**, 58–61.
14 J. Wang and R. Ding, *Inorganics*, 2018, **6**, 11.
15 A. Shojaeian, *J. Mol. Liq.*, 2017, **229**, 591–598.
16 S. Aparicio, M. Atilhan and F. Karadas, *Ind. Eng. Chem. Res.*, 2010, **49**, 9580–9595.
17 M. S. Aminuddin, Z. Man, M. A. Bustam Khalil and B. Abdullah, *E3S Web Conf.*, 2021, **287**, 02003.
18 J.-G. Lu, Y.-F. Zheng and D.-L. He, *Sep. Purif. Technol.*, 2006, **52**, 209–217.

19 P. K. Mohapatra, *Dalton Trans.*, 2017, **46**, 1730–1747.
20 O. Brettschneider, R. Thiele, R. Faber, H. Thielert and G. Wozny, *Sep. Purif. Technol.*, 2004, **39**, 139–159.
21 Y. Zhao, J. Gao, Y. Huang, R. M. Afzal, X. Zhang and S. Zhang, *RSC Adv.*, 2016, **6**, 70405–70413.
22 H. Sakhaeinia, A. H. Jalili, V. Taghikhani and A. A. Safekordi, *J. Chem. Eng. Data*, 2010, **55**, 5839–5845.
23 M. Han and R. M. Espinosa-Marzal, *ACS Appl. Mater. Interfaces*, 2019, **11**, 33465–33477.
24 C. Chiappe and C. S. Pomelli, in *Ionic Liquids II*, Springer, 2017, pp. 265–289.
25 C. Wang, Y. Guo, X. Zhu, G. Cui, H. Li and S. Dai, *Chem. Commun.*, 2012, **48**, 6526–6528.
26 F. Ding, J. Zheng, Y. Chen, K. Chen, G. Cui, H. Li and C. Wang, *Ind. Eng. Chem. Res.*, 2014, **53**, 18568–18574.
27 J. O. Valderrama and K. Zarricueta, *Fluid Phase Equilib.*, 2009, **275**, 145–151.
28 P. Wasserscheid and T. Welton, *Ionic liquids in synthesis*, John Wiley & Sons, 2008.
29 H. F. Almeida, J. A. Lopes-da-Silva, M. G. Freire and J. A. Coutinho, *J. Chem. Thermodyn.*, 2013, **57**, 372–379.
30 Y. Cao and T. Mu, *Ind. Eng. Chem. Res.*, 2014, **53**, 8651–8664.
31 J. Wang and W. Zhang, *Energy Fuels*, 2014, **28**, 5930–5935.
32 G. Srinivas, S. C. Gebhard and D. W. DeBerry, *Hybrid sulfur recovery process for natural gas upgrading*, National Energy Technology Laboratory (NETL), Pittsburgh, PA, Morgantown, WV, 2001.
33 M. D. Nguyen, L. V. Nguyen, E. H. Jeon, J. H. Kim, M. Cheong, H. S. Kim and J. S. Lee, *J. Catal.*, 2008, **258**, 5–13.
34 M. L. Samaniego, M. D. G. de Luna, D. C. Ong, M.-W. Wan and M.-C. Lu, *Energy Fuels*, 2019, **33**, 1098–1105.
35 X. Liu and R. Wang, *Fuel Process. Technol.*, 2017, **160**, 78–85.
36 M. H. Ibrahim, M. Hayyan, M. A. Hashim and A. Hayyan, *Renewable Sustainable Energy Rev.*, 2017, **76**, 1534–1549.
37 A. W. Bhutto, R. Abro, S. Gao, T. Abbas, X. Chen and G. Yu, *J. Taiwan Inst. Chem. Eng.*, 2016, **62**, 84–97.